POST LOCAL BUCKLING BEHAVIOR AND PLASTIC ROTATION CAPACITY OF STEEL BEAM-COLUMNS

by Isao MITANI(I) and Minoru MAKINO(II)

SUMMARY

Theoretical analysis of the post local buckling behavior of a wide-flange member is first performed. The results of analysis show good agreement with the cyclic behavior obtained by the tests. Second, empirical formulae estimating the rotation capacity of beam-columns are established, mainly based on the experimental results. Good agreement between experimental and predicted values of rotation capacity is observed, and it is shown that the formulae are valid for the members under arbitrary moment gradients.

INTRODUCTION

It is well known that restoring force of a steel member is deteriorated owing to the lateral and/or local buckling, and therefore, in the design of frames against strong earthquake motion, it is essential to clarify inelastic behavior of the locally buckled members. Many experimental studies on the post local and/or lateral buckling behavior of wide-flange steel members have been performed. But very few theoretical studies were done[1]. In the plastic design, it is needed that the members possess sufficient rotation capacity. Therefore, for the development of reasonable design methods, correlation between the plastic rotation capacity and various essential factors has to be clarified. However, very few researches were done[2, 3].

In this paper, the analysis of the post local buckling behavior of steel beam-columns based on the plastic limit theorem is first performed, and the results are compared with the experimental results[4. 5]. Second, empirical formulae estimating plastic rotation capacity that contain several essential parameters are established.

THEORETICAL ANALYSIS

A theoretical analysis is performed on the post local buckling behavior of wide-flange beam-columns shown in Fig.1(a). The analysis is mainly based on the technique used in Ref.[1]. However, the present analysis takes into account effects of plastic elongation in a local hinge forming in the plate element, and effects of axial stresses in the plate element on a specific power of dissipation of the local hinge.

BASIC EQUATIONS AND ASSUMPTIONS At the plastic hinge rotating as shown in Fig.1, the principle of virtual velocities and the principle of maximum specific power of dissipation[6] give

$$M\cdot\dot{\theta} + P(\eta - 0.5)d\cdot\dot{\theta} = Dp \qquad (1)$$

where M = applied moment at the plastic hinge, P = constant axial load, ηd = distance between the flange compressed in the virgin loading cycle and the neutral axis as illustrated in Fig.2, d = web depth, $\dot{\theta}$ = virtual angular velocity of the plastic hinge, and Dp = total power of dissipation(= rate of

(I) Lecturer, Faculty of Engineering, Kagoshima Univ., Kagoshima, Japan.
(II) Professor, Faculty of Engineering, Kyushu Univ., Fukuoka, Japan.

internal energy dissipation) at the plastic hinge. From Eq.(1), resisting moment M is obtained as

$$M = -P(\eta - 0.5)d + D_P/\dot{\theta} \qquad (2)$$

For simplicity, the following assumptions are used. 1° Relative strains at a plastic hinge are proportional to the distance from the neutral axis(Fig.2). 2° Member is composed of a rigid-perfectly-plastic material. 3° Plate elements are in state of plane stress, and yielding or buckling occurs when the yield condition of von Mises is satisfied, i.e.,

$$\Phi = \sigma_x^2 + \sigma_y^2 - \sigma_x\sigma_y + 3\tau^2 - Y^2 = 0 \qquad (3)$$

where σ_x and σ_y = normal stresses in x and y directions, respectively, τ = shear stress, and Y = yield stress in simple tension. 4° Deformations are sufficiently small. 5° Strain reversals in one loading cycle do not occur. 6° A kinematically admissible velocity field in the plastic hinge with local buckling is assumed as illustrated in Fig.3, in which the deformation is confined to the heavy lines and the hatched regions. 7° A kinematically admissible velocity field in the local hinge is assumed as indicated in Fig.4(b). 8° Strain rates are specified by the flow rule, i.e.,

$$\dot{\varepsilon}_x = \lambda(\partial\Phi/\partial\sigma_x), \qquad \dot{\varepsilon}_y = \lambda(\partial\Phi/\partial\sigma_y), \qquad \dot{\gamma} = \lambda(\partial\Phi/\partial\tau) \qquad (4)$$

where λ = arbitrary nonnegative factor of proportionality, $\dot{\varepsilon}_x$, $\dot{\varepsilon}_y$, and $\dot{\gamma}$ = generalized strain rates corresponding to σ_x, σ_y, and τ, respectively.

Power of dissipation in a plastic region is generally defined by

$$\int_V (\sigma_x\dot{\varepsilon}_x + \sigma_y\dot{\varepsilon}_y + \tau\dot{\gamma})\,dV \qquad (5)$$

where the integration is extended over the entire continuum.

POWER OF DISSIPATION IN A LOCAL HINGE [D_H] Figure 4 shows an idealized plate element with local plastic hinge. The plate element is subjected to average stress $\bar{n}Y$, the angle between axis of the local hinge and plate center axis is ϕ, and the stresses in the local hinge are defined as shown in Fig.4 (a). When the local hinge rotates under the velocity $\dot{\rho}$, the assumptions that the length does not change and plane remains plane after the deformations take place lead to

$$\dot{\varepsilon}_y = 0 \qquad (6), \qquad \dot{\varepsilon}_x^{\pm} = \pm|\dot{\rho}|/2 \qquad (7)$$

where superscripts + and - denote quantities on compression and tension sides in the local hinge, respectively. In view of von Mises condition(Eq.(3)), stress components appearing in Eq.(5) are determined from the equilibrium of forces acting on an infinitesimal element shown in Fig.4(a), and the equilibrium of forces in the cross section of the local hinge shown in Fig.4 (b). In view of strain rates given in Eqs.(6) and (7), together with the flow rule, Eq.(4), integrating Eq.(5) leads to the expression of D_H, i.e.,

$$\frac{D_H/\dot{\theta}}{bdfY} = \frac{1}{8\sqrt{3}}\frac{\ell t^2}{bdf}\left[4 + \frac{3\bar{n}^2\sin^4\phi}{1-A}\right]\frac{|\dot{\rho}|/\dot{\theta}}{\sqrt{1-A}} \qquad (8)$$

where t = plate thickness, 2b and f = flange width and thickness, respectively, ℓ = length of local hinge, and $A = 3(\bar{n}\cdot\sin\phi\cdot\cos\phi)^2$. The angular velocity $\dot{\rho}$ is related to the angular velocity at the fixed end $\dot{\rho}_a$, as

$$\dot{\rho} = C_\rho\cdot\dot{\rho}_a \qquad (9)$$

where C_ρ takes a constant value depending on the value of ϕ. When the line S'S"(or D'D") in Fig.3 is assumed to be a rectangular bar fixed at both ends, the following is obtained by considering the geometory of the deflected bar.

$$\rho_a\cdot\dot{\rho}_a = \dot{\varepsilon}_a - \dot{\varepsilon}_h \qquad (10)$$

where ρ_a and $\dot{\rho}_a$ = rotation and angular velocity of plastic hinge forming at both ends of the bar, respectively, and $\dot{\varepsilon}_a$ and $\dot{\varepsilon}_h$ = relative axial strain

rate of the bar and its plastic component, respectively. Note that $\dot{\varepsilon}_a$ contains the component due to change in geometry by the deflection(see Eq.(19)). $\dot{\rho}_a$ and $\dot{\varepsilon}_h$ are related by the flow rule. From the assumptions 1° and 6°, $\dot{\varepsilon}_a$ is expressed by

$$\dot{\varepsilon}_a = C_H \cdot d \cdot \dot{\theta}/(2\zeta b) \qquad (11)$$

where C_H is a function of the variable η, and $2\zeta b$ is a length shown in Fig.3. In view of Eqs.(10) and (11), and the flow rule, $\dot{\rho}_a$ in Eq.(9) is computed as

$$\dot{\rho}_a = [C_H \cdot d/(2\zeta b)] \cdot [\dot{\theta}/\{\rho_a + t|n|/(\zeta b)\}] \qquad (12)$$

where $|n| = (\sqrt{\delta^2 + 1} - \delta)$ = ratio of axial load carried by the bar to the axial yield load, when the deflection at the center of the bar becomes equal to $\delta \cdot t$.

POWER OF DISSIPATION IN A REGION WITH SIMULTANEOUS AXIAL AND ROTATIONAL DEFORMATIONS [D_S] Stresses in a region that is deforming axially with out-of-plane deformation are defined as shown in Fig.3(b). The line S'S"(or D'D") in Fig.3 is assumed again to be the rectangular bar fixed at both ends. Then, the following equations are obtained in this region.

$$\tau = 0 \qquad (13), \qquad \dot{\varepsilon}_x = C_S \cdot \dot{\varepsilon}_a \qquad (14)$$

where C_S is a function of η. Substituting Eq.(11) into Eq.(14) yields.

$$\dot{\varepsilon}_x = C_H \cdot C_S \cdot d \cdot \dot{\theta}/(2\zeta b) \qquad (15)$$

As a result of a rigid plate element rotating about a local hinge, the plastic deformation occurs in the adjacent plate element. For example, the rigid plate $\square$AKLS in Fig.3(b) rotates about the local hinge AK, and the plastic deformations occur in the plate ΔASB, satisfying the following condition.

$$\dot{\varepsilon}_h - \dot{\varepsilon}_a = \beta^2 \cdot \dot{\varepsilon}_y \qquad (16)$$

where $\beta = \tan\psi$, ψ being the angle $\angle$ABS. The relation given by Eq.(16) must be held in the web plate, ΔADB and ΔEDF, where $\beta = \tan\kappa$, κ being the angle $\angle$ABD in Fig.3(a). In view of Eqs.(3), (4), (13), (15), and (16), quantities in Eq.(5) are determined, and D_S is obtained as follows;

$$\text{For } \frac{\dot{\varepsilon}_x}{C_S} \gtrless 0, \quad \frac{D_S/\dot{\theta}}{bdfY} = \pm \frac{C_H}{\sqrt{3}} \cdot \frac{t}{f} \cdot \frac{\zeta}{\beta} \sqrt{\alpha^2 + \alpha[C_S\beta^2 - 2] + C_S{}^2\beta^4 - C_S\beta^2 + 1} \qquad (17)$$

where $\alpha = \dot{\varepsilon}_h/\dot{\varepsilon}_a = 1 - (\delta/\sqrt{\delta^2 + 1})$

POWER OF DISSIPATION IN A REGION REMAINING IN PLANE [D_N] The regions such as ΔECF in Fig.3(a) may deform under $|\sigma_x| = Y$ and $\sigma_y = \tau = 0$. Therefore, power of dissipation D_N in such regions can be obtained easily.

METHOD OF ANALYSIS The power of dissipation in each plastic region (D_H, D_S, and D_N) can be computed when the deflections at point S of both flanges and at point D of the web are given in addition to the parameters η, ζ, and ψ that specify the collapse mechanism. D_P in Eq.(2) is obtained by the sum of the power of dissipation in each plastic region. Variation of the rotation $\Delta\theta$ measured from the point of load reversal, such as points ① , ② , ····· , ④ in Fig.2, is computed by

$$\Delta\theta = 2\zeta b(\Delta\varepsilon^c - \Delta\varepsilon^t)/(d + f) \qquad (18)$$

where, $\Delta\varepsilon$ = variation of axial strain at the center of a flange thickness measured from the point of load reversal, superscripts c and t indicate the strain of the flanges in compression and tension at the virgin loading cycle, respectively.

$\Delta\varepsilon^c$ is equal to $\Delta\varepsilon_a$ that is the variation of relative axial strain, measured from the point of load reversal at S'S" in the compression flange at the virgin loading cycle, and $\Delta\varepsilon^t$ is of the tension flange in the same

sense. $\Delta\varepsilon_a$ may be decomposed into geometric component $\Delta\varepsilon_g$ and plastic component $\Delta\varepsilon_h$. $\Delta\varepsilon_g$ is given by

$$\Delta\varepsilon_g = (\delta^2/2)\cdot(t/\zeta b)^2 - (\varepsilon_g)_0 \qquad (19)$$

where $(\varepsilon_g)_0$ = value of geometric strain component at the point of load reversal. From the yield condition for the rectangular cross section and the associated flow rule, the following relation is obtained.

$$\dot{\varepsilon}_h = [t|n|/(\zeta b)]\cdot\dot{\rho}_a \qquad (20)$$

Noting that ρ_a is a function of n, and $(\dot{})$ in Eq.(20) can be considered as a differentiation with respect to n, integration by parts gives the expression for $\Delta\varepsilon_h$ as follows[7];

$$\Delta\varepsilon_h = [t/(2\zeta b)]^2\cdot[2\ell n|n| - 2\ell n|n_0| + n^2 - n_0{}^2] \qquad (21)$$

where n_0 = value of n at the point of load reversal.

This analysis is based on the upper bound theorem. Therefore, among the M - θ relations, the lowest result is valid. In the numerical computation, the values of ζ and ψ are tacitly assumed to be constant. For a specified value of the deflection at point S of the one flange, the value of η is determined from the condition $\partial M/\partial\eta = 0$ which satisfies the lowest solution for M. Note that the deflections of other portion of the plastic hinge are determined to satisfy the assumption 1°.

COMPARISON WITH EXPERIMENTAL RESULTS Two examples of the analysis are shown in Figs.5(a) and (b) by solid curves, where the values of ζ and ψ are assumed constant to be 0.4 and π/4 rad., respectively. It was verified numerically that those values gave the lowest or nearly the lowest value of M at $\theta/\theta_{pc} = 5$, where M_{pc} and θ_{pc} denote the full plastic moment and the elastic limit rotation, respectively, considering the effects of the axial load. From the comparison of solid curves with dashed curves that denote experimental results[4, 5], it is observed that the analysis well predicts the experimental behavior with the local buckling. However, for the specimens with slender plates, the analytical curves overestimate the load carrying capacity.

The mode indicated in Fig.3 is one of the simplest modes for the alternating bending. For the member under the monotonic loading, models shown in Fig.(6) give also kinematically admissible velocity fields, in which the buckling mode of the flange is the same as the one shown in Fig.3. The analytical results obtained by the similar procedure mentioned above, based on the models shown in Figs.6(a) and (b), are indicated by dotted curves and dash-dotted curves, respectively, in Fig.5. Comparing with three kinds of analytical curves, it is found that the collapse mechanism assumed for alternating bending gives greater load carrying capacity than the ones for monotonic bending, and that the collapse mechanism without web buckling gives often the lowest load carrying capacity in the range of the small value of θ.

EMPIRICAL FORMULAE ESTIMATING ROTATION CAPACITY

For a moment-rotation relation of the steel member as illustrated in Fig.7, the plastic rotation capacity of the member is generally defined by

$$R = (\theta_{cr}/\theta_{pc}) - 1 \qquad (22)$$

where θ_{cr} = critical rotation defined by θ_m or $\theta_{0.95}$ as shown in Fig.7. Previous researches have shown that the plastic rotation capacity of the steel members with local and/or lateral buckling is related to various factors. From investigation on the independency of those factors, it is found that

the following parameters are considered to be essential and independent; Y, $\lambda_f = (b/f)\sqrt{Y/E}$, $\lambda_w = (D/w)\sqrt{Y/E}$, ℓ_x/i_x, k, ℓ_b/i_y, and P/P_y. In the parameters above, E = modulus of elasticity, D = depth of a cross section, w = web thickness, ℓ_x = length between the plastic hinge and the point of zero moment, ℓ_b = unbraced length, k = effective length factor for the lateral buckling, i_x and i_y = radii of gyration about strong and weak axes, respectively, and Py = yield axial load.

EQUIVALENT PLASTIC ROTATION CAPACITY AND EMPIRICAL FORMULA In order to derive the empirical formula, it is first considered that the real rotation capacity R is given in the form of (R_{eq})x(a function of ℓ_x/i_x, ℓ_b/i_y, k, Y), where Req is the equivalent plastic rotation capacity defined as a fictitious plastic rotation capacity that is a function of λ_f and λ_w only. In Ref.[3], the empirical formula

$$R = (i_y/\ell_b)\sqrt{F/Y} \cdot (\text{function of cross sectional sizes}) \qquad (23)$$

is suggested, where F = 2.4 ton/cm^2. This formula is based on the test results under the condition, $\ell_x = \ell_b$. To investigate the effect of ℓ_x/i_x, the post local buckling behavior of cantilever beam-columns is analyzed taking the collapse mode shown in Fig.6(b), and the results are plotted in Fig.8, defining θ_{cr} in Eq.(22) as the rotation at $M/M_{pc} = 1.0$. Figure 8 indicates that R - ℓ_x/i_x relation may be expressed by

$$R = C \cdot i_x/\ell_x - 1.0 \qquad (24)$$

where C is a constant depending on the factors except for ℓ_x/i_x. Taking the form of Eqs.(23) and (24) into the consideration, the following formula is obtained by the method of trial and error.

$$R = \sqrt{\frac{500}{k(\ell_x/i_x)\cdot(\ell_b/i_y)} \cdot \frac{F}{Y}} \cdot (Req) \qquad (25)$$

The procedure to determine R_{eq} as a function of λ_f and λ_w is as follows. First, the values of Req are computed from Eq.(25) by substituting the test results[4, 5] of the rotation capacity observed at $\theta_{cr} = \theta_m$ into R, and they are plotted against arguments of λ_f and λ_w. Sample results for the case $P/P_y = 0$ are shown in Figs.9 and 10. In this computation, k is taken equal to 0.7, since all test specimens in Refs.[4 and 5] are cantilever beam-columns, whose out-of-plane deflections are restrained at the top. Note that the value of k becomes 1.0, if the simply supported beam-columns are considered(Fig.11). Figs.9 and 10 indicate that Req - λ_f - λ_w relations may be expressed by

$$R_{eq} = C_1(\lambda_f - C_2)^2 + C_3\lambda_w + C_4 \quad ; \quad C_1 \sim C_4 = \text{constants} \qquad (26)$$

Substituting Eq.(26) with the values of $C_1 \sim C_4$ determined by the method of trial and error into Eq.(25) leads to

$$\text{For } P = 0, \quad R = \sqrt{\frac{500}{k(\ell_x/i_x)(\ell_b/i_y)} \cdot \frac{F}{Y}} \cdot [80(\lambda_f - 0.65)^2 - 4.0\lambda_w + 6] \qquad (27a)$$

$$\text{For } P \neq 0, \quad R = \sqrt{\frac{500}{k(\ell_x/i_x)(\ell_b/i_y)} \cdot \frac{F}{Y}} \cdot [50(\lambda_f - 0.65)^2 - 5.5\lambda_w + 7] \qquad (27b)$$

The formulae above are valid in the range $\lambda_f < 0.65$.

DISCUSSION In Figs.12 and 13, the experimental values of the rotation capacity R_{exp} appearing in Refs.[2 ~ 5, 8, and 9] are compared with the predicted values R_{pred} by Eq.(27). The test conditions in each reference are shown in Table 1. It is observed from Figs.12 and 13 that more than 70%(for P = 0) and 80%(for P ≠ 0) of the experimental values lie in the range, $R_{pred} - 2 < R_{exp} < R_{pred} + 2$. For examining valid range of Eq.(27a), two values of

R_{pred} are calculated by Eqs.(27a) and (27b), and plotted in Fig.14. It seems that Eq.(27a) is valid in the range $0 < P/P_y < A_w/2A$, where A_w is area of the web, and A is area of the cross section.

The formulae are also applicable to the case $M_2 \neq 0$, although Eq.(27) is established based on the test results under the condition $M_2/M_1 = 0$, where M_1 and M_2 are values of bending moments at the lateral supports, and $|M_2| < |M_1|$. To show the validity, consider the ratio of R to $\tilde{R}$ that is the value of R under the condition $M_2 = 0$, if the bending moment distribution is linear,

$$\ell_x = \ell_b/(1.0 - M_2/M_1) \tag{28}$$

In view of Eqs.(27) and (28), the ratio $R/\tilde{R}$ is obtained as

$$R/\tilde{R} = \sqrt{(1.0 - M_2/M_1)\cdot\tilde{k}/k} \tag{29}$$

where $\tilde{k}$ = value of k under the condition $M_2 = 0$. $\tilde{k}$ is related to k as

$$k/\tilde{k} = \sqrt{1.75/C_b} \tag{30}$$

where $C_b = 1.75 - 1.05(M_2/M_1) + 0.3(M_2/M_1)^2$ and < 2.3.
In Fig.15, (M_2/M_1) - $(R/\tilde{R})$ relations based on Eq.(29) are plotted together with an empirical formula presented in Ref.[10]. The dotted and dash-dotted curves are both obtained from Eq.(29), the former taking $k/\tilde{k} = 1.0$ regardless of the values of k, and the latter using Eq.(30). From Fig.15, it is observed that the influence of the bending moment gradients on the plastic rotation capacity is well estimated, even though the value of $k/\tilde{k}$ is simply assumed to be 1.0, regardless of the values of M_2/M_1.

CONCLUSION

It is shown that the post local buckling behavior of wide-flange beam-columns subjected to alternating bending is well predicted by the analysis based on the plastic limit theorem for rigid-perfectly-plastic material. Empirical formulae estimating the plastic rotation capacity of the steel member under monotonic bending are established, and shown that the experimental results are well predicted by the formulae which contain several parameters.

ACKNOWLEDGMENTS

The study presented in this paper was done as a part of the project " Restoring Force Characteristics of Steel Frames with Local Buckling" sponsored by the Ministry of Education, Japan. Principal investigators involved are Assoc. Prof. C. Matsui of Kyushu Univ. and the authors. The authors wish to express profound gratitude to him for the stimulating discussions and criticisms. Acknowledgment is extended to Assoc. Prof. S. Morino of Kyushu Univ. for the comments given during the preparation of this paper.

REFERENCES

[1] J. J. Climenhaga and R. P. Johnson : MOMENT-ROTATION CURVES FOR LOCALLY BUCKLING BEAMS, ASCE, Vol.98 ST 6, June 1972, pp. 1239-1254.
[2] B. Kato, H. Akiyama, and Y. Obi : DEFORMATION CHARACTERISTICS OF H-SHAPED STEEL MEMBERS INFLUENCED BY LOCAL BUCKLING, Trans. of Architectural Institute of Japan, No.257, July 1977, pp. 49-58 (in Japanese).
[3] T. Suzuki, T. Ono, and Y. Kanebako : THE LOCAL BUCKLING AND INELASTIC DEFORMATION CAPACITY OF STEEL BEAMS UNDER SHEAR BENDING, Trans. of A.I.J., No.260, Oct. 1977, pp. 91-98 (in Japanese).
[4] I. Mitani and et al. : INFLUENCE OF LOCAL BUCKLING ON CYCLIC BEHAVIOR OF STEEL BEAM-COLUMNS, Proc. of 6th WCEE, New Dehli, Jan. 1977, pp.3175-3180.
[5] M. Makino and et al. : POST LOCAL BUCKLING BEHAVIOR OF STEEL BEAM-COLUMNS, Trans. of A.I.J., No.281, July 1979, pp. 71-80 (in Japanese).

[6] W. Prager : AN INTRODUCTION TO PLASTICITY, Addison-Wesley, 1959.
[7] M. Wakabayashi, T. Nonaka, and N. Yoshida : ELASTIC - PLASTIC BEHAVIOR OF A RESTRAINED STEEL BAR UNDER CYCLIC AXIAL LOADING, Proc. of Kinki Branch Convention of A.I.J., June 1976, pp. 197-201 (in Japanese).
[8] Y. Fukuchi and M. Ogura : EXPERIMENTAL STUDIES ON LOCAL BUCKLING AND HYSTERETIC CHARACTERISTICS OF H-SHAPE BEAMS, Trans. of A.I.J., No.228, Feb. 1975, pp. 65-71 (in Japanese).
[9] T. Suzuki and T. Ono : EXPERIMENTAL STUDIES ON THE PLASTIC DESIGN ON HIGH-STRENGTH STEEL BEAMS, Trans. of A.I.J., No.219, May 1974, pp. 39-45 (in Japanese).
[10] T. Suzuki and T. Ono : EXPERIMENTAL STUDY OF THE PLASTIC STEEL BEAM (2) (Beam under Moment Gradient), Trans. of A.I.J., No.171, May 1970, pp. 31-36 (in Japanese).

FIGURES AND TABLE

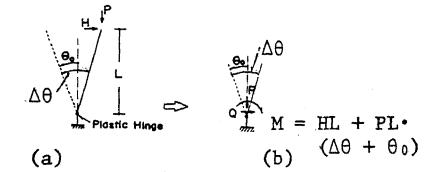

Fig. 1 Model of Analysis

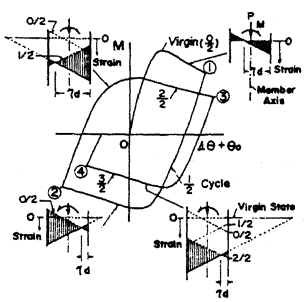

Fig. 2 M - θ Curve and Variation of Strain

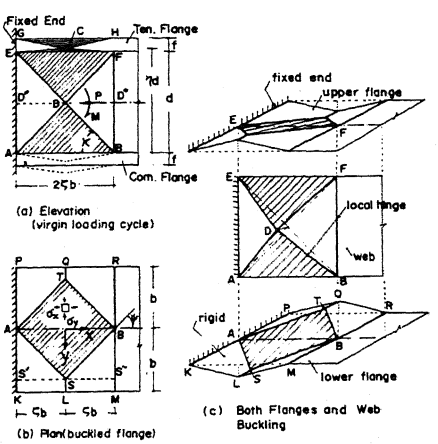

Fig 3 Local Buckling Mechanism (Cyclic Loading)

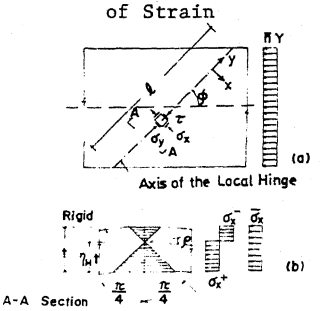

Fig. 4 Stresses in the Local Plastic Hinge

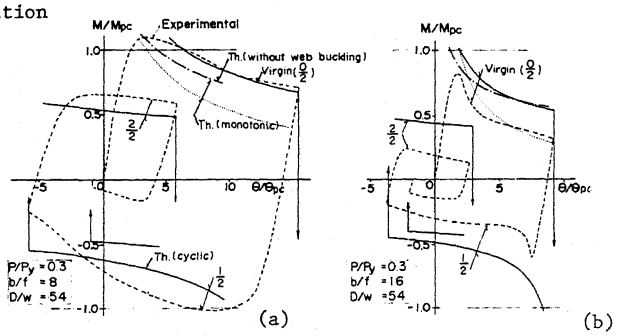

Fig. 5 Comparison between Experimental and Theoretical Results

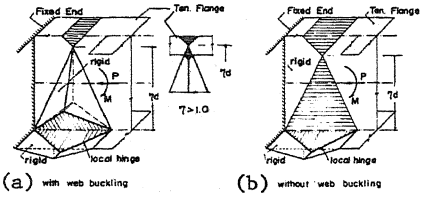

Fig. 6 Local Buckling Mechanism (Monotonic Loading)

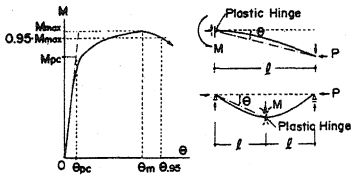

Fig. 7 M–θ Relation and Definition of Critical Rotation

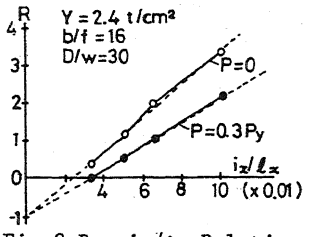

Fig 8 R – i_x/ℓ_x Relations

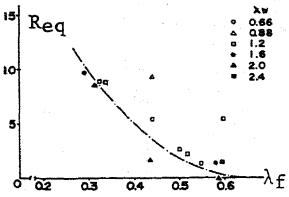

Fig 9 R_{eq} – λ_f Relations

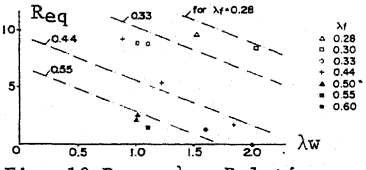

Fig. 10 R_{eq} – λ_w Relations

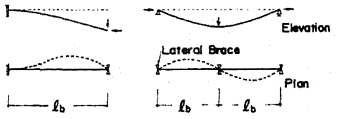

Fig. 11 Out-of-Plane Deflections

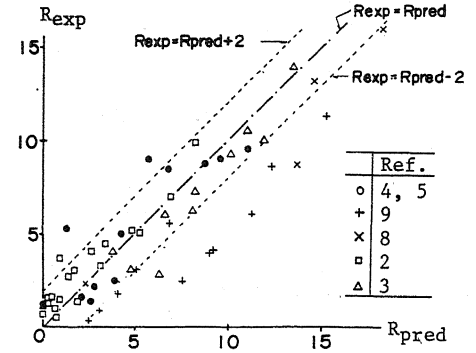

Fig. 12 Comparison between R_{exp} and R_{pred} (P=0)

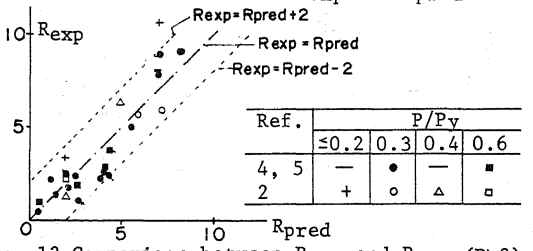

Fig. 13 Comparison between R_{exp} and R_{pred} ($P \neq 0$)

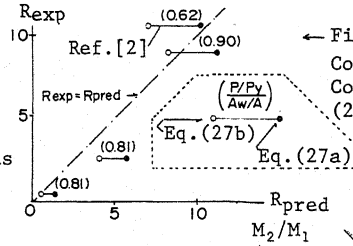

← Fig. 14 Comparison of R_{pred} Computed by Eqs. (27a) and (27b)

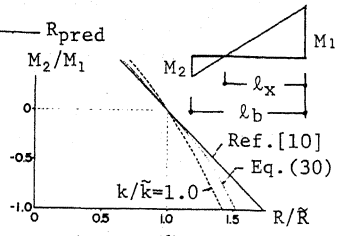

Fig. 15 M_2/M_1 – $R/\tilde{R}$ Relations

Table 1 Range of Parameters in the Tests

Ref.	Y(t/cm²)	λ_f	λ_w	ℓ_b/i_y	ℓ_x/i_x
2	2.6~5.3	.27~.61	0.76~2.8	32~125	5~29
3	2.7	.28	1.1 ~3.3	29~ 55	7~13
4,5	2.4~4.7	.23~.61	0.59~2.4	28~ 61	12~20
8	2.7~2.8	.29~.55	0.91~1.4	13~ 22	10~11
9	3.2~8.8	.20~.34	0.82~1.4	45~ 76	12~21